A NEM SZIMMETRIKUS MEGTÁMASZTÁS HATÁSA GÖRBE RUDAK STABILITÁSÁRA

THE INFLUENCE OF NON-SYMMETRICAL SUPPORTS ON THE STABILITY OF ARCHES

Messaoudi Abderrazek, László Péter Kiss**, Krzysztof Murawski****

ABSTRACT

A cikk keretein belül körívalakú görbe rudak stabilitását vizsgáljuk, amennyiben a megtámasztás nem szimmetrikusan történik. A rúd az egyik végén csuklóval támasztott, a másik végén befalazott. Terhelése egy radiális irányú koncentrált erőből áll. A geometriailag nemlineáris mechanikai modell stabilitási egyenletei a virtuális munka elvből kerültek levezetésre, megoldásuk zárt alakban felírható. Az egyensúlyi utak feltérképezésével megállapítható a legkisebb limit ponti kritikus erő, ami a rúd stabilitásának elvesztéséhez vezethet. Az új modell eredményeit kereskedelmi végeselemes szoftver számításaival összevetve jó egyezést tapasztaltunk.

1. INTRODUCTION

Arches are frequently utilized in various architectural designs, serving as essential elements in structures like roofs, bridges, and openings. Their distinctive curved shape offers several advantages, notably in distributing weight evenly and effectively managing mechanical loads. Nevertheless, when arches endure a compressive load, they can become prone to instability and it is crucial to account for the possibility of limit point buckling in arch design to guarantee structural stability and safety [1]. Buckling of arches has been widely studied, resulting in a rich body of literature that provides key insights into the stability of arch structures, from early research to present-day. According to certain numerical studies, including those by Yang & Shieh [2], Kuo & Yang [3], the position of the radial load may influence the nonlinear equilibrium and buckling load significantly. Numerous studies have primarily focused on the classical and nonlinear buckling of arches with symmetric boundary conditions, particularly those with pinned-pinned or fixed-fixed ends – see, e.g., [4–7]. Exact analytical solutions for limit point, bifurcation buckling, and post-buckling behaviour of the shallow arches with symmetric boundary conditions under uniform radial and central concentrated loads have been investigated in details in the literature. Recent studies on arches with unsymmetrical end supports have revealed significant differences in their nonlinear behaviour compared to arches with symmetric conditions. Likewise, paper [8] examined the in-plane nonlinear stability of pinned-fixed shallow arches under arbitrary concentrated loads and found that these structures exhibit multiple stable and unstable equilibria, buckling through limit point instability rather than bifurcation. This contrasts with fixed-fixed or pinned-pinned arches, which may buckle in a bifurcation mode [5,7]. Nonlinear elastic analysis and buckling of pinned-fixed arches under uniformly distributed radial loads were also explored in [9]. In most articles, the effect of bending moment on the membrane strain is not incorporated, but it might be necessary to improve the model accuracy [10].

Overall, most studies assume identical end supports and overlook the impact of bending moments on membrane strain when analyzing the buckling behaviour of arches. Therefore, further investigation into the stability of such members is needed to provide a more comprehensive understanding of their buckling behaviour. This article focuses on the in-plane buckling of homogeneous fixed-pinned shallow arches under radial concentrated load. The equilibrium equations are derived using the principle of virtual work, with account on the bending moment's effect on membrane strain. The equations are solved in closed form. The novel model introduced can identify the limit points on the equilibrium path for a selected geometry, material and load position. The solutions are validated through comparisons with finite element simulations.

** PhD candidate, University of Miskolc, Institute of Applied Mechanics*
*** associate professor, University of Miskolc, Institute of Applied Mechanics*
**** former senior lecturer, Jacob Paradies University, Gorzów*

2. MECHANICAL MODEL

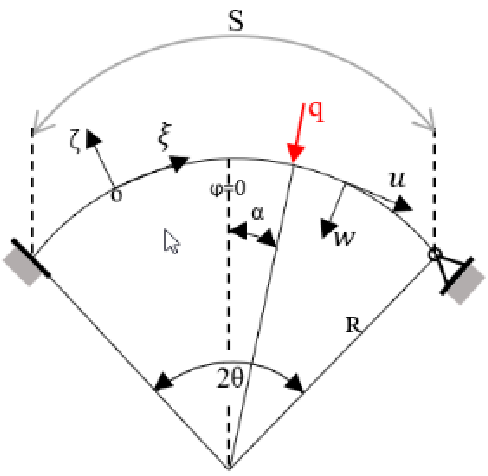

Figure 1 The geometry, loading and support conditions of the one-dimensional model

We shall consider a fixed-pinned arch as it is shown in Figure 1. The cross-sectional coordinates are $\eta; \zeta$ and the axis ξ coincides with the circumferential direction. The length of the arch is S, the included angle is 2θ, the initial radius of curvature is R, and φ and s are the angle and arc coordinates. The load is applied at the angle coordinate $\alpha = [-\theta; \theta]$. If $\alpha = 0$, it is a limit case with the load being at the symmetry axis of the arch. It is assumed that the behaviour of the material is linearly elastic and isotropic.

The membrane strain at an arbitrary point on the centroidal axis ($\zeta = 0$) is given as [11]

$$\varepsilon_m = \frac{du}{ds} + \frac{w}{R} + \frac{1}{2}\left(-\frac{dw}{ds}\right)^2 \quad . \tag{1}$$

Where u and w are the axial and radial centroidal axis displacements respectively, the nonlinear term $(-\frac{dw}{ds})^2$ is introduced to account for rotations and it contributes as the cause of nonlinearity. The axial force N and the bending moment M can be represented as follows [10] using the Hooke law:

$$N = A_e\varepsilon_m - \frac{I_e}{R}\left(\frac{du}{Rds} - \frac{d^2w}{ds^2}\right), \tag{2}$$

$$M = -I_e\left(\frac{d^2w}{d^2s} + \frac{w}{R^2}\right), \quad N = A_e\varepsilon_m - \frac{M}{R} \tag{3}$$

with I_e as the E-weighted moment of inertia to major principal axis η and and A_e as the E-weighted area of the cross-section:

$$I_e = \int E\zeta^2 dA\,, \qquad A_e = \int_A E\, \mathrm{d}A. \tag{4}$$

Using the principle of virtual work, the nonlinear pre-buckling equilibrium configuration can be established.

For mathematical simplification, we now introduce $W = \frac{w}{R}$ and $U = \frac{u}{R}$ that are dimensionless normal and circumferential displacements. Using fundamental equations (1)–(4), the following equilibrium equations can be found [7]:

$$\varepsilon_m{}' = 0, \;\; W''' + (\varsigma^2 + 1)W'' + \varsigma^2 W = \varsigma^2 - 1 \tag{5}$$

with $\frac{d(\square)}{ds} = (\square)'$,

$$\varsigma^2 = 1 - \mu\varepsilon_m \;,\; \mu = \frac{A_e.R^2}{I_e} = \frac{R^2}{r^2}, \lambda = \sqrt{\mu}\,\Theta^2 = \frac{S^2}{4rR} \tag{6}$$

In which λ is the slenderness parameter of the arch [11] and r is the radius of gyration of the cross section about its major principal axis η. The boundary and discontinuity conditions for the considered arch are as follows:

$$W|_{\varphi=-\theta} = W'|_{\varphi=-\theta} = W|_{\varphi=\theta} = W''|_{\varphi=\theta} = 0,$$
$$W|_{\varphi=-\alpha.} = W|_{\varphi=+\alpha} \;;\; W'|_{\varphi=-\alpha} = W'|_{\varphi=+\alpha} \;,$$
$$W''|_{\varphi=-\alpha} = W''|_{\varphi=+\alpha} \,, -W'''|_{\varphi=-\alpha} + W'''|_{\varphi=+\alpha} = -\frac{2Q}{\theta}. \tag{7}$$

Here Q is a dimensionless load defined by

$$Q = \frac{qR^2\theta}{2I_e}. \tag{8}$$

When we focus, example, on that arch part which is on the right side of the load position ($\varphi \in [\alpha, \Theta]$), the general solution satisfying Eq (5)$_2$ is

$$W_r(\varphi) = \frac{\varsigma^2 - 1}{\varsigma^2} + A_1\cos(\varphi) + A_2\sin(\varphi) - \frac{A_3}{\varsigma^2}\cos(\varsigma\varphi) - \frac{A_4}{\varsigma^2}\sin(\varsigma\varphi). \tag{9}$$

The constants A_i can be found by recalling boundary and discontinuity conditions (7).

Since the membrane strain is constant, a nonlinear relationship can be set as

$$\int_{-\Theta}^{\Theta}\varepsilon_m(\varphi)d\varphi \simeq \int_{-\Theta}^{\Theta}[U' + W + 0.5(W')^2]d\varphi - 2\mu\varepsilon_m = B_1\,Q^2 + B_2 Q + B_3. \tag{10}$$

The constants B_1, B_2 and B_3 -- which are functions of α, θ, λ and μ -- can be calculated in closed form based on their definitions. Evaluation of Eq. (10) makes it possible to find the equilibrium path of the arch and thus, the limit points which are related to buckling.

3. COMPUTATIONAL RESULTS

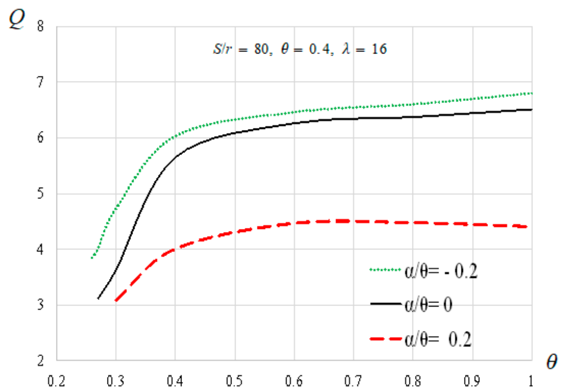

Figure 2 Lowest critical load in terms of θ

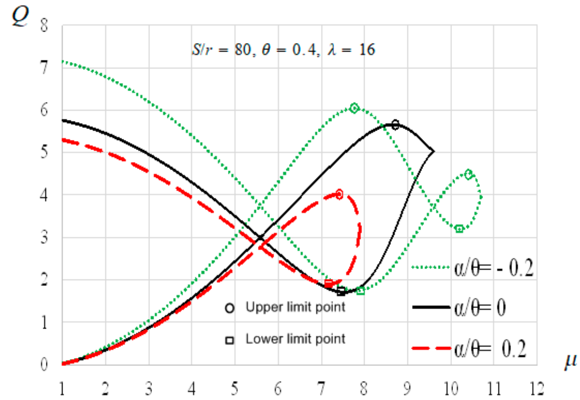

Figure 3 Load in terms of a dimensionless strain μ

Figure 2 depicts the relationship between dimensionless buckling loads and the semi-vertex angle θ for three various load positions. The results reveal that when the load position factor is negative, the critical load increases as θ increases, indicating that arches with greater θ can sustain higher loads. Conversely, for a strictly positive load position factor, the critical load initially rises but begins to decrease once θ approaches to approximately *0.81* rad. Additionally, when the load is applied between the crown and the fixed end, the buckling load is significantly higher compared to when the load is located between the crown and the pinned end. The plotted curves also shift leftward as the load position factor α/θ transitions from positive to negative, meaning buckling may occur at smaller included angles. The difference in critical load is substantial, with the relative change between $\alpha/\theta = -0.2$ and $\alpha/\theta = 0.2$ ranging between *30.8*% and *35.14*%. It is important to note that, under the considered geometric parameters and these load positions, the critical buckling load for pinned-fixed members consistently falls between the values for pinned-pinned [10] and fixed-fixed supports [5].

The effects of the load position on the equilibrium path (number of limit points and nonlinear equilibrium branches) are illustrated in Figure 3 for three samples. The load position α/θ clearly influences the nonlinear equilibrium and buckling behaviour of the arches. As the load position shifts from the left side of the arch crown ($\alpha/\theta = -0.2$) to the right ($\alpha/\theta = 0$ and $\alpha/\theta = 0.2$), the number of limit points decreases from four (two upper limit points and two lower limit points) to two. Similarly, the equilibrium branches reduce from five (one primary stable branch, three unstable branches, and a remote stable branch) to three (two stable branches with an unstable branch between them).

4. FEM RESULTS

Table 1 presents a comparison between the proposed model and the results obtained with the commercial finite element (FEM) software Abaqus. For the FEM analysis, a one-dimensional *B21* type element was employed for the discretization, with a total of *60* elements to map the arch. This number was found to be sufficient to ensure converged results. The Static/Riks step was utilized with nonlinear geometry enabled to trace the equilibrium paths. The first upper limit point of the equilibrium path is obtained when the force reaches its local maximum and then starts to decrease under load control. Accordingly, this maximum force is the lowest nonlinear buckling load sought. The cross-section used was a uniform, doubly symmetric I cross-section with an area of $4588\ mm^2$ and a second moment of inertia being $54255295\ mm^4$. The Young's modulus was *210* GPa throughout, meaning homogeneous material distribution. As shown in Table 1, the correlation is really good between the two different approaches.

Table 1 Validation of the results with FEM

	Q (new model)	FEM
α/θ	*S/r=80,* $\theta = 0.4$, $\lambda = 16$	
-0.2	6.03	5.85
0	5.65	5.41
0.2	4.01	3.90

Furthermore, Figures 4 and 5 illustrate the pre-buckling shape of the arch when the critical buckling load in [N] is applied when $\alpha/\theta = -0.2$ and 0.2, respectively. To determine the corresponding dimensionless loads in the above table, the definition of Eq. (8) was applied.

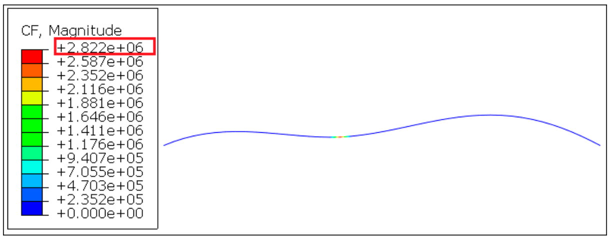

Figure 4 Critical load when $\alpha/\theta = -0.2$

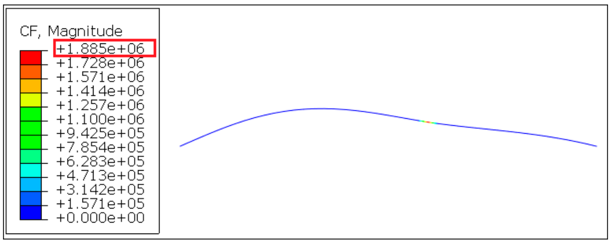

Figure 5 Critical load when $\alpha/\theta = 0.2$

5. SUMMARY

This article investigates the stability and in-plane behaviour of fixed-pinned shallow circular arches using a one-dimensional beam model based on the Euler-Bernoulli theory. It turns out that not only the geometry but also the load position affects significantly the lowest buckling loads. The equilibrium path also strongly depends on these factors. Comparative studies with finite element analyses validate the accuracy of the model.

6. REFERENCES

[1] TIMOSHENKO S. P., GERE J. M.: *Theory of Elastic Stability*. Engineering Societies Monographs, 1961.

[2] YANG Y. B., SHIEH M. A.: Solution method for nonlinear problems with multiple critical points", *AIAA Journal* 28(12), (1990), 2110–2116. https://doi.org/10.2514/3.10529

[3] KUO S. R., YANG Y. B.: Tracing postbuckling paths of structures containing multi loop. *International Journal of Numerical Methods in Engineering* 38(23), (1995), 4053–4075. https://doi.org/10.1002/nme.1620382309

[4] BRADFORD M. A., UY B., PI Y.-L.: In-plane elastic stability of arches under a central concentrated load. *Journal of Engineering Mechanics*, 128 (7), (2006), 710-719. https://doi.org/10.1061/(ASCE)0733 9399(2002)128:7(710)

[5] PI Y.-L., BRADFORD M. A., LIU A.: Nonlinear equilibrium and buckling of fixed shallow arches subjected to an arbitrary radial concentrated load. *International Journal of Structural Stability and Dynamics* 17(8), (2017). Art. No. 1750082. https://doi.org/10.1142/S0219455417500821

[6] MESSAOUDI A., KISS L. P.: Investigation on the limit-point buckling of curved beams. *Multidiszciplináris Tudományok* (Multidisciplinary Sciences), 13 (2), (2023), 78–86. https://doi.org/10.35925/j.multi.2023.2.7

[7] KISS L. P.: Nonlinear stability analysis of FGM shallow arches under an arbitrary concentrated radial force. *International Journal of Mechanics and Materials in Design,* 16 (2020), 91-108. https://doi.org/10.1007/s10999-019-09460-2

[8] LIU A., BRADFORD M. A., PI Y.-L.: In-plane nonlinear multiple equilibria and switches of equilibria of pinned–fixed arches under an arbitrary radial concentrated load. *Archives of Applied Mechanics* 87, (2017), 1909–1928. https://doi.org/10.1007/s00419-017-1300-7

[9] PI Y.-L., BRADFORD M. A.: Nonlinear elastic analysis and buckling of pinned–fixed arches. *International Journal of Mechanical Sciences* 68 (2013),212–223. https://doi.org/10.1016/j.ijmecsci.2013.01.018

[10] KISS L., SZEIDL G.: Nonlinear in-plane stability of heterogeneous curved beams under a concentrated radial load at the crown point. *Technische Mechanik*. 35(1), (2015), 1–30. https://doi.org/10.24352/UB.OVGU-2017-066

[11] BRADFORD M. A., UY B., PI Y.-L.: In-plane stability of arches. *International Journal of Solids and Structures*, 39 (1), (2002), 105-125. https://doi.org/10.1016/S0020-7683(01)00209-8